THE JOURNAL OF PHYSICAL CHEMISTRY B

Article

pubs.acs.org/JPCB

A New Amphipathic, Amino-Acid-Pairing (AAP) Peptide as siRNA Delivery Carrier: Physicochemical Characterization and in Vitro Uptake

Mousa Jafari,[†,‡,∥] Wen Xu,[†,‡,∥] Sheva Naahidi,[†,‡,§] Baoling Chen,[†,‡] and P. Chen*[,†,‡]

[†]Department of Chemical Engineering, University of Waterloo, Waterloo, ON, N2L 3G1, Canada

[‡]Waterloo Institute for Nanotechnology, University of Waterloo, ON, Canada

[§]Harvard-MIT Division of Health Sciences and Technology, Massachusetts Institute of Technology, Cambridge, Massachusetts 02139, United States

ABSTRACT: RNA interference has emerged as a powerful tool in biological and pharmaceutical research; however, the enzymatic degradation and polyanionic nature of short interfering RNAs (siRNAs) lead to their poor cellular uptake and eventual biological effects. Among nonviral delivery systems, cell-penetrating peptides have been recently employed to improve the siRNA delivery efficiency. Here we introduce an 18-mer amphipathic, amino-acid-pairing peptide, C6, as an siRNA delivery carrier. Peptide C6 adopted a helical structure upon coassembling with siRNA. The C6-siRNA coassembly showed a size distribution between 50 and 250 nm, confirmed by dynamic light scattering and atomic force microscopy. The C6-siRNA interaction enthalpy and stoichiometry were 8.8 kJ·mol^{-1} and 6.5, respectively, obtained by isothermal titration calorimetry. A minimum C6/siRNA molar ratio of 10:1 was required to form stable coassemblies/complexes, indicated by agarose gel shift assay and fluorescence spectroscopy. Peptide C6 showed lower toxicity and higher efficiency in cellular uptake of siRNA compared with Lipofectamine 2000. Fluorescence microscopy images also confirmed the localization of C6-siRNA complexes in the cytoplasm using Cy3-labeled siRNAs. These results indicate high capabilities of C6 in forming safe and stable complexes with siRNA and enhancing its cellular uptake.

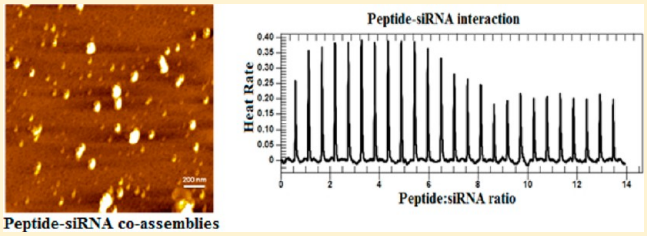

INTRODUCTION

The field of gene therapy has witnessed significant expansion over the past decades. The discovery of RNA interference (RNAi) offered the main contribution to this growth. RNAi is a highly regulated process, in which double-stranded, short interfering RNA (siRNA) cleaves the complementary mRNA, causing posttranscriptional gene silencing (PTGS).[1] This sequence-specific gene knockdown eventually hinders the production of the target protein in a highly specific manner. This exceptional feature of RNAi makes it a valuable tool in studying gene function and signaling pathways as well as developing siRNA-based pharmaceutical agents.

However, despite abundant promise, the translation of RNAi to realistic therapeutics has faced serious obstacles. The large size and polyanionic nature of free siRNAs prevent them from translocating across the negatively charged cell membrane. Moreover, without protection, siRNAs are subject to enzymatic degradation under physiological conditions. These highlight the importance of developing an efficient siRNA delivery system, which can (i) interact with siRNA and condense it into small nanoparticles, (ii) protect siRNA against degradation, (iii) cross the cell membrane, and (iv) release siRNA to the target site, that is, cytosol. Several nonviral siRNA delivery systems, including polymers,[2−4] lipids,[5−7] and peptides,[8−12] have been developed for this purpose.

Cell-penetrating peptides (CPPs), net positively charged peptides with fewer than 30 amino acids, have been widely applied to deliver cargos into cells. Despite numerous reports on CPPs' high efficiency, their cellular uptake mechanism is still under debate. Several pathways including energy-dependent endocytosis[13,14] and direct translocation[15,16] have been proposed as the major uptake mechanism of CPPs. The interaction of CPP with the cargo can occur through either chemical linkage or noncovalent forces. Considering the negatively charged backbone of siRNA, the noncovalent electrostatic interaction is usually preferred to obtain stable peptide−siRNA complexes without any need for chemical linkage or modification of siRNA.

Considering the amphiphilic nature of the cell membrane, most CPPs possess both hydrophilic and hydrophobic moieties. The hydrophilic side interacts with the hydrophilic heads of the lipid bilayer and hydrophilic drugs/genes through electrostatic interaction, whereas the hydrophobic side is anchored in the hydrophobic core of the bilayer, triggering the endocytosis pathways or assisting the direct translocation of peptide-cargo to the cytosol. The amphiphilicity of the peptides may evolve

Received: July 22, 2012
Revised: October 4, 2012
Published: October 18, 2012

dx.doi.org/10.1021/jp3072553 | J. Phys. Chem. B 2012, 116, 13183−13191

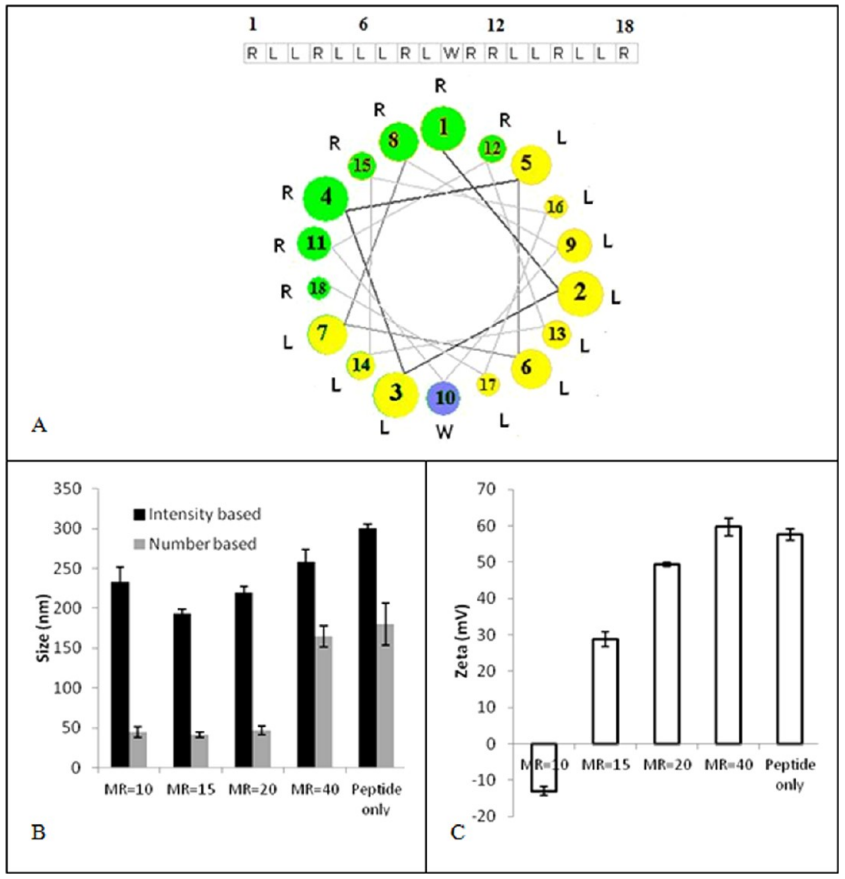

Figure 1. (A) Helical wheel projection of peptide C6. A downward cross-sectional view of the α helix axis, orthogonal to the paper plane, is shown. The bigger the circle is, the upper turn the residue is located at, when viewing from the top. R (green), L (yellow), and W (blue) represent arginine, leucine and tryptophan residues, respectively. Size (B) and zeta potential (C) of C6-siRNA complexes at different molar ratios. The siRNA concentration was 100 nM, and the peptide concentration in "peptide only" sample was 4 μM. Three independent measurements were performed for each sample 20 min after sample preparation at 25 °C. Error bars represent the standard deviation of three replicates. (MR = peptide/siRNA molar ratio).

from their primary structure, for example, MPG,[17] or secondary structure, for example, penetratin,[18] and CADY.[12] In the latter case, the peptide needs to adapt a helical structure to organize hydrophilic and hydrophobic moieties at different sides of the peptide.[12,18]

Over the past several years, we have been studying the concept of amino acid pairing (AAP) and have established principles to design peptides to form a variety of stable nanostructures, such as fibers, rods, tubes, and globules.[11,19−22] Different mechanisms including electrostatic, hydrogen bonding, hydrophobic, and $\pi-\pi$ stacking are incorporated in peptide assembly. Applying this strategy, we designed the 18-amino-acid peptide, C6, as siRNA delivery carrier.

Three types of amino acids were incorporated in the design of C6 peptide (Ac-RLLRLLLRLWRRLLRLLR-NH_2): (i) Seven arginine residues were incorporated to interact with siRNA and cell membrane. Positively charged arginine residues can interact with the negatively charged phosphate groups on the siRNA backbone via ionic interactions. These basic residues also interact with negatively charged cell surface proteoglycans to initiate their cellular uptake.[23] CPPs with six to nine arginine residues have been reported to have the highest translocation efficiency.[24] (ii) Ten leucine residues were incorporated to induce the amphiphilicity and helicity to the peptide structure. These hydrophobic residues are found abundantly in the helical regions of proteins.[25] They also interact with hydrophobic tails of lipid bilayer and facilitate the translocation of peptide.[26] (iii) An aromatic tryptophan residue in the middle of the sequence was incorporated to use as an intrinsic fluorescence probe to study the structural change of peptide upon changing the environment or interaction with siRNA.

Because each turn of a peptide helix includes 3.6 residues, arginine residues were distributed along the peptide sequence in three or four residue intervals, so when a helical structure was formed, they all faced the same side of the helix (Figure 1A). This induces amphiphilicity to the peptide structure as polar (R) and nonpolar (L,W) residues face opposite sides when peptide adopts a helical structure. This arrangement of amino acids facilitates the self-assembly of peptide, mainly through hydrophobic interaction of leucine faces of helices. Furthermore, the presence of all arginine residues on hydrophilic face of the helix facilitates ionic interaction of positively charged residues with siRNA backbone, maximizing the loading capacity of the peptide.

The article will be focused on physicochemical characterization of C6 and its coassembly/complex with siRNA as well as C6-mediated cellular uptake of siRNA using several biophysical, spectroscopy, and microscopy approaches.

EXPERIMENTAL METHODS

Peptide and siRNA. The C6 peptide (Ac-RLLRLLLRLWRRLLRLLR-NH_2, MW = 2470.2 g/mol) was

dx.doi.org/10.1021/jp3072553 | J. Phys. Chem. B 2012, 116, 13183−13191

purchased from CanPeptide (Quebec, Canada). High-performance liquid chromatography (HPLC) analysis indicated that the synthetic peptide was at least 98% pure. The unlabeled (AM4624) and 5′ cy3 dye-labeled glyceraldehyde 3-phosphate dehydrogenase (GAPDH) siRNA (AM4649) were purchased from Ambion (Austin, TX). The siRNA used in agarose gel electrophoresis and fluorescence spectroscopy is eGFP siRNA, which was purchased from Dharmacon with an extinction coefficient of 362 408 L/mol cm. The sense sequence is GACGUAAACGG CCACAAG UUC and antisense sequence is ACUUGUGGCCGU UUACGUCGC.

Cell Culture. The CHO-K1 (Chinese hamster ovary) cells were purchased from American Type Culture Collection (ATCC CCL-61). Cells were cultured in F-12K (Thermo Scientific, Ottawa, Canada) supplemented with 10% FBS (Sigma-Aldrich, Oakville, Canada). Cells were incubated at 37 °C in a humidified atmosphere containing 5% CO_2.

Preparation of Peptide−siRNA Coassembly/Complex. The C6 peptide was prepared by dissolving peptide powder in RNase-free water. A stock solution of 1 mM was made and diluted at desirable concentrations for various experiments. The solution was vortexed for 10 s and sonicated for 10 min in a tabletop ultrasonic cleaner (Branson, model 2510). siRNA was diluted in RNase-free water to a concentration of 50 μM. Peptide−siRNA complexes were formed by adding peptide solution into siRNA in proportion according to the designed experiment. The complexes were incubated for 20 min at room temperature before each experiment.

Dynamic Light Scattering (DLS) and Zeta Potential. The hydrodynamic diameters of the peptide C6 self-assemblies/aggregates (4 μM) and the C6-siRNA coassemblies/complexes were measured on a Zetasizer Nano ZS (Malvern Instruments) equipped with a 4 mW He−Ne laser operating at 633 nm. Samples at molar ratios of 10:1, 20:1, and 40:1 with final siRNA concentration of 100 nM were prepared, as previously mentioned. A quartz microcell (45 μL) with a 3 mm light path was used, and the scattered light intensities were collected at an angle of 173°. Clear disposable zeta cells were used for zeta potential measurements. The intensity-based size distribution and zeta potential values were acquired using the multimodal algorithm CONTIN, Dispersion Technology Software 5.0. Three independent measurements were performed for each sample 20 min after sample preparation at 25 °C.

Atomic Force Microscopy (AFM). The nanostructures of peptide C6 (40 μM) and C6-siRNA (molar ratio of 40:1) complexes were characterized by AFM. The sample solution (10 μL) was placed on a freshly cleaved mica surface, fixed on a glass slide, and incubated for 30 min at room temperature to allow the sample to adhere onto the mica surface. The mica was then rinsed five times with Milli-Q water to remove any unattached particles, followed by air-drying overnight. The mica surface was analyzed by a PicoScan AFM (Molecular Imaging, Phoenix, AZ) at room temperature using the tapping mode with silicon single-crystal tips (NCL type, Molecular Imaging), with a typical tip radius of 10 nm and resonance frequency of <170 kHz. A scanner with the maximum scan size of 5 μm × 5 μm was used. All AFM images were obtained at a resolution of 512 × 512 pixels on a scale of 2 μm × 2 μm.

Circular Dichroism (CD) Spectroscopy. Spectra from 250 to 190 nm with spectral resolution and pitch of 1 nm and scan speed of 200 nm/min were recorded with a J-810 spectropolarimeter (Jasco). Increasing amounts of siRNA were added to a fixed peptide concentration of 20 μM to obtain different molar ratios. Samples were transferred into 1 mm long quartz cells and maintained at 25 °C. Spectra shown are the average of three replicates.

Isothermal Titration Calorimetry. Isothermal titration calorimetry (ITC) experiments were conducted on a Nano-ITC calorimeter (TA Instruments) with a cell volume of 174 μL. The peptide C6 (250 μM) and siRNA (6 μM) were prepared in RNase-free water. All samples were degassed in a degassing station (TA Instruments) prior to experiments. Milli-Q water was used in the ITC reference cell. For each titration, 2 μL of the peptide in a pipet stirring at 300 rpm was automatically added to siRNA solution in the sample cell of the calorimeter, equilibrated at 25 °C, with an interval of 300s between injections. The heat of dilution was measured by titrating C6 solution into RNase free water and subtracted from the measured sample heat. A single-site independent model was used to determine the binding constant (K), the stoichiometry (n), and the binding enthalpy (ΔH) using NanoAnalyze software v.2.3.0. The change in free energy (ΔG) and entropy (ΔS) were calculated using the equations $\Delta G = -RT \ln K$ and $\Delta G = \Delta H - T\Delta S$, respectively, where R is the gas constant, T is the absolute temperature, and K is the equilibrium constant.

Agarose Gel-Shift Assay. The ability of C6 to coassemble with siRNA was investigated by agarose gel (1.2 wt %/vol) shift assay. siRNA was incubated for 30 min at 37 °C in RNase-free water with different concentrations of C6 to obtain peptide/siRNA molar ratios ranging from 1:1 to 80:1. The samples (10 μL containing 0.3 μg of siRNA per well) and loading dye were loaded to each well, and electrophoresis was carried out at a constant voltage of 55 V for 1.5 h in TBE buffer (4.45 mM Tris−base, 1 mM sodium EDTA, 4.45 mM boric acid, pH 8.3) containing 0.5 μg/mL ethidium bromide.

In the case of heparin competition assay (Figure 4A), different amounts of heparin corresponding to final concentrations from 0.5 to 10 μg heparin per 10 μL of complex were added to C6/siRNA complexes at molar ratios of 15:1, 40:1, 60:1, and 80:1. Ten microliters of each sample, corresponding to 50 pmol of siRNA, was then analyzed by electrophoresis on agarose gel (1.2 wt %/vol) stained with ethidium bromide.

Fluorescence Spectroscopy. Because the peptide C6 has a tryptophan (Trp) residue, which is an important intrinsic fluorescent probe, fluorescence spectroscopy was applied as a powerful technique to characterize the interaction between siRNA and peptide. The peptide fluorescence was acquired on a Photon Technology International spectrafluorometer (Type LS-100, London, Canada) with a pulsed xenon lamp as the light source. Samples (80 μL) were transferred to a quartz cell (1 cm × 1 cm) and excited at 280 nm, and spectra were collected in the range of 300−500 nm. The standard fluorescence intensity I_s was obtained by taking the average of the fluorescence of C6-only sample from 480 to 500 nm. Different volumes of siRNA stock solution were added to the fixed peptide concentration of 160 nM to obtain peptide/siRNA molar ratio from 80:1 to 1:1.

Cy-3-labeled siRNA was also used as an extrinsic fluorescent probe, and the change in fluorescence spectra was studied at a fixed concentration of siRNA (2 μM) and increasing concentration of peptide to achieve different molar ratios. The samples were excited at 540 nm, and spectra were collected in the range of 550−800 nm. The spectra were normalized by taking I_s as the average of the fluorescence of Cy-3 siRNA-only sample from 780 to 800 nm.

Cytotoxicity. CHO-K1 cells were used for in vitro cellular toxicity studies of C6 and C6-siRNA complexes. Cells were detached from the flasks by adding trypsin-EDTA and incubating for 5 min, centrifuging at 500 rpm for 5 min, and resuspending in fresh cell culture media at a concentration of 6 × 10^4 cells per mL. Cell suspension (100 μL) was added to each well of a flat-bottomed 96-well plate and incubated for 24 h. The media was then replaced with fresh media with different final concentrations of C6 or C6-siRNA complex or control (Lipofectamine 2000). The cell-counting kit-8 (CCK-8) (Dojindo, Japan) was used to perform cytotoxicity assays 48 h post-treatment. CCK-8 substrate (10 μL) was added to each well and incubated for an additional 2 h at 37 °C in the dark. Absorbance was measured at a wavelength of 450 nm with a reference wavelength of 620 nm using a microplate reader (FLUOstar OPTIMA, BMG, NC).

Fluorescence-Activated Cell Sorting (FACS). The amount of Cy-3 labeled siRNA uptaken by the cells was studied by Flow Cytometry (type BD Biosciences, BD FACSVantage SE Cell Sorter, USA). Approximately 50 000 CHO-K1 cells were seeded in a 24-well cell culture plate 24 h before treatment. Cy3-labeled GAPDH siRNA was complexed with C6 peptide at molar ratios of 15:1, 25:1, and 40:1 and incubated at room temperature for 20 min. Lipofectamine 2000 (Invitrogen) was complexed with labeled siRNA according to manufacturer's protocol and used as a positive control. The complexes were added to cells with a final siRNA concentration of 50nM per well and incubated at 37 °C for 3 h in Opti-MEM (Invitrogen). The medium was removed by aspiration, and the wells were washed with heparin (10 U/mL, three times total for 1 h at 37 °C). After washing, the cells were detached from the plate by adding trypsin-EDTA and resuspended in fresh 4% paraformaldehyde (PFA) in phosphate-bufferred saline (PBS) and collected in FACS tubes for analysis.

Fluorescence Microscopy. To investigate the distribution of the C6-siRNA complexes in CHO-K1 cells, we used Cy-3-labeled siRNA. CHO-K1 cells were treated with C6-Cy3siRNA complexes at molar ratios of 15:1 and 40:1 or Lipofectamine 2000 at 37 °C for 3 h in Opti-MEM, as previously described. The medium was discarded, and the wells were washed with PBS and heparin and fixed with 500 μL/well of fresh 4% PFA solution for 30 min. The fixation agent was aspirated, and the cells were washed twice with PBS and covered with Fluoroshield with DAPI solution (Sigma-Aldrich, Oakville, Canada) to stain the cell nuclei. The samples were visualized using an inverted fluorescence microscope (Zeiss AxioObserver Z1, Canada). Images were analyzed using AxioVision software package.

RESULTS AND DISCUSSION

Complex Size, Morphology, and Zeta Potential. The particle size and charge significantly affect its circulation in the bloodstream, biodistribution, and uptake by the cells. The particle size ranging from 100 to 500 nm would be ideal for passive targeting to solid tumors through the enhanced permeability and retention (EPR) effect.[27−29] The size can also dictate the pathway of cellular uptake.[30] It was also reported that highly charged particles can be recognized by the reticuloendothelial system (RES) more rapidly than neutral or slightly charged particles.[31,32] Therefore, engineering the nanoparticle to obtain appropriate physical properties could significantly enhance its therapeutic effect.

Figure 1B,C shows the average intensity and number-based size and zeta potential of C6-siRNA coassemblies at different molar ratios. The intensity-based data are highly influenced by the presence of large particles, even though they are a few in the solution. Number-based data represent the size distribution of particles based on their population. For monodisperse particles, these two values should be almost identical. However, the intensity-based average size is always higher than that of number-based in polydisperse particles.

As shown in Figure 1B, the majority of C6-siRNA coassemblies at molar ratios of 10:1 to 20:1 had an average size of ∼50 nm. However some larger particles (∼200 nm) were also observed. The size of complexes was increased by adding more peptides because the extra peptides added layers to the initially formed peptide−RNA cores. This finding was in agreement with AFM images (Figure 2A), which shows the

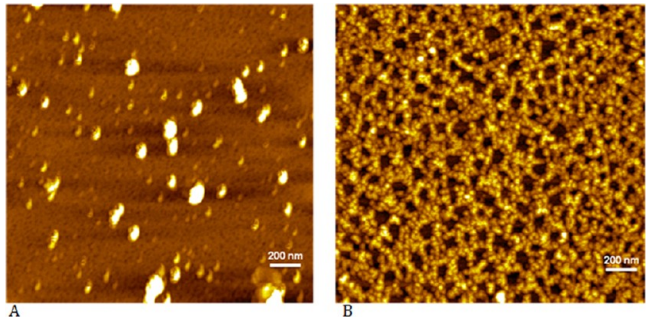

Figure 2. AFM images of (A) C6-siRNA complex (MR = 40:1) and (B) C6 peptide aggregates/assemblies (40 μM). The sample solution (10 μL) was placed on the mica surface and incubated for 30 min at room temperature. The mica was then rinsed five times with Milli-Q water, followed by air-drying overnight. The scan size of the images is 2 × 2 μm^2.

high population of small nanoparticles (∼50 nm) as well as the presence of larger complexes (∼100−200 nm). At molar ratio of 40:1, the complex became more uniform as the intensity and number-based DLS results showed the average size between 150 and 250 nm.

The peptide-only sample formed aggregates of 200−300 nm in solution; however, on the mica surface (Figure 2B), the peptide sample formed globular structures with an average diameter of ∼45 nm, eventually organized to form a network of strings of nanospheres. The formation of these globular structures was derived by hydrophobic attraction between leucine residues, distributed along the peptide sequence. Because there was not such a template for nanoparticles in solution in DLS experiment to form the network, they aggregated, instead, as larger particles to minimize the interaction of hydrophobic residues and water molecules. This self-assembly/aggregation process is thermodynamically favored by minimizing Gibbs free energy through limiting the exposure of hydrophobic residues to the aqueous environment and having mostly charged arginine residues on the surface of globules. We have already reported similar morphology for another AAP peptide.[33]

The surface charge of C6-siRNA complex at molar ratio of 10:1 was slightly negative, which implies that siRNA molecules were not fully saturated by peptides (Figure 1C). Considering seven positively charged arginine groups of the peptide C6 and 21 pairs of negatively charged nucleotides in a siRNA molecule, it was theoretically expected to neutralize the negative charge of

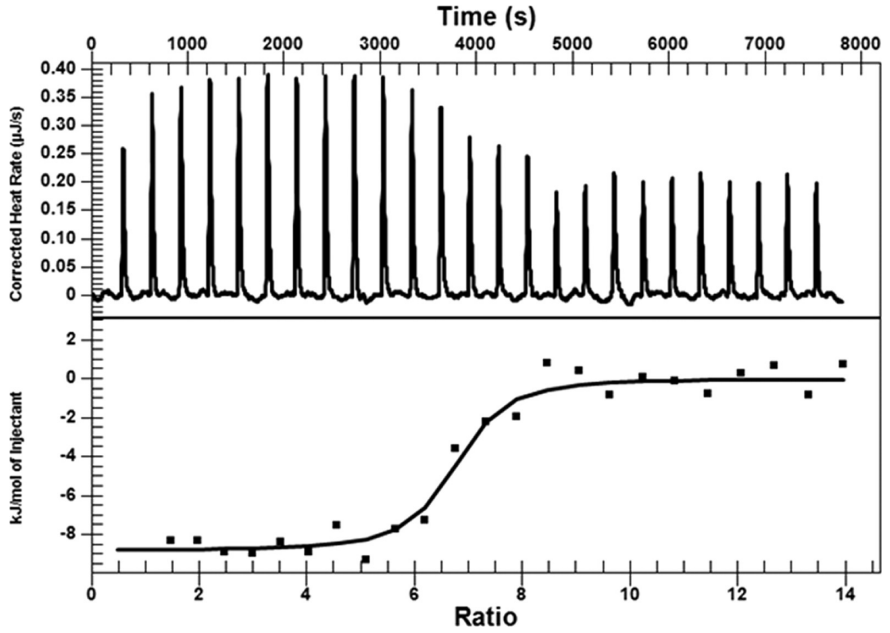

Figure 3. Titration of 250 μM peptide C6 into the solution of 6 μM siRNA. The upper panel shows the baseline-corrected thermogram of released heat at each injection, and the lower graph shows the integrated areas of the net heat of each titration after subtracting the heat of the dilution of peptide to water as a function of the molar ratio of peptide to siRNA. A single site-independent model was used for fitting the data points (solid curve in lower panel).

Table 1. Thermodynamic Parameters of the Interaction between Peptide and siRNA

stoichiometry	K (10^6 M^{-1})	ΔH (kJ/mol)	$T\Delta S$ (kJ/mol)	ΔG (kJ/mol)
6.49 ± 0.33	9.23 ± 0.63	−8.86 ± 0.55	30.95 ± 1.14	−39.81 ± 1.69

siRNA at molar ratio of 6:1; however, at a higher molar ratio, that is, 15:1, the zeta potential of the complex jumped to +30 mV, indicating that peptides fully covered the surface of the complex. With the increasing concentration of peptide at the same siRNA concentration, the positive value of the surface charge of the complexes increased from +30 (MR = 15:1) to +60 mV (MR = 40:1) due to the increase in the number of positively charged arginine residues. The net positive charge of the particles is crucial because it inhibits particle aggregation and enhances electrostatic interaction with the negatively charged phospholipids of the cell membrane upon siRNA delivery.

Peptide−siRNA Coassembly Detected by ITC. To study the thermodynamic aspects of C6-siRNA interaction, we used ITC to detect the heat exchanged during the titration of siRNA with C6 solution.

As shown in Figure 3, the interaction between C6 and siRNA created small exothermic peaks, followed by a gradual decrease in the exchanged heat after the first several injections. The heat measured for the last injections was almost the same as the dilution heat (control experiment), implying that there was no significant interaction after saturation ratio. The thermodynamic parameters of the interaction were obtained by fitting the raw ITC data to a single-site model (Table 1).

Interestingly, the obtained molar stoichiometry of ~6.5 was very close to the theoretical one, that is, 6. With a low enthalpy of 8.8 kJ·mol^{-1}, the binding was mostly entropy driven, with a ΔS of 103 J·mol^{-1}·K^{-1}, which contributes to 78% of the binding free energy. This type of thermodynamic parameters, that is, low enthalpy and high positive entropy values, is consistent with a typical charge neutralization or ionic interaction process, for example, the interaction of basic amino acids with RNA[34] or DNA.[35]

It should be noted that the thermodynamic parameters of the interaction are strong functions of experimental conditions, for example, temperature, pH, and ionic strength. The values reported here were the results of experiments conducted in water (pH 6) at 25 °C.

Agarose Gel Shift Assay. Agarose gel shift assay was used to detect the interaction between siRNA and peptide molecules and the stability of the formed complex in the presence of heparin. Peptide can interact with siRNA through noncovalent interactions such as Coulombic forces and hydrogen bonding. In particular, basic amino acids such as lysine, arginine, or histidine can interact with the negatively charged phosphate groups on the siRNA sugar rings through electrostatic interactions. Free siRNA molecules could move toward the positive electrode when the voltage is applied, whereas the inability of peptide−siRNA complexes to enter the agarose gel suggests the formation of stable complex with no free siRNAs to be shown in siRNA bands.

As shown in Figure 4B, the effective formation of the peptide−siRNA complex started at molar ratio of as low as 5:1 because the band was less bright than that of siRNA only. At the molar ratio of 10:1, siRNA molecules were almost completely associated with peptide C6 because a very small amount of free siRNA was observed on siRNA band. This band was completely disappeared at the molar ratio of 15:1. This finding suggests that excess peptide molecules are needed to obtain stable peptide/RNA complexes as six molecules of

dx.doi.org/10.1021/jp3072553 | J. Phys. Chem. B 2012, 116, 13183−13191

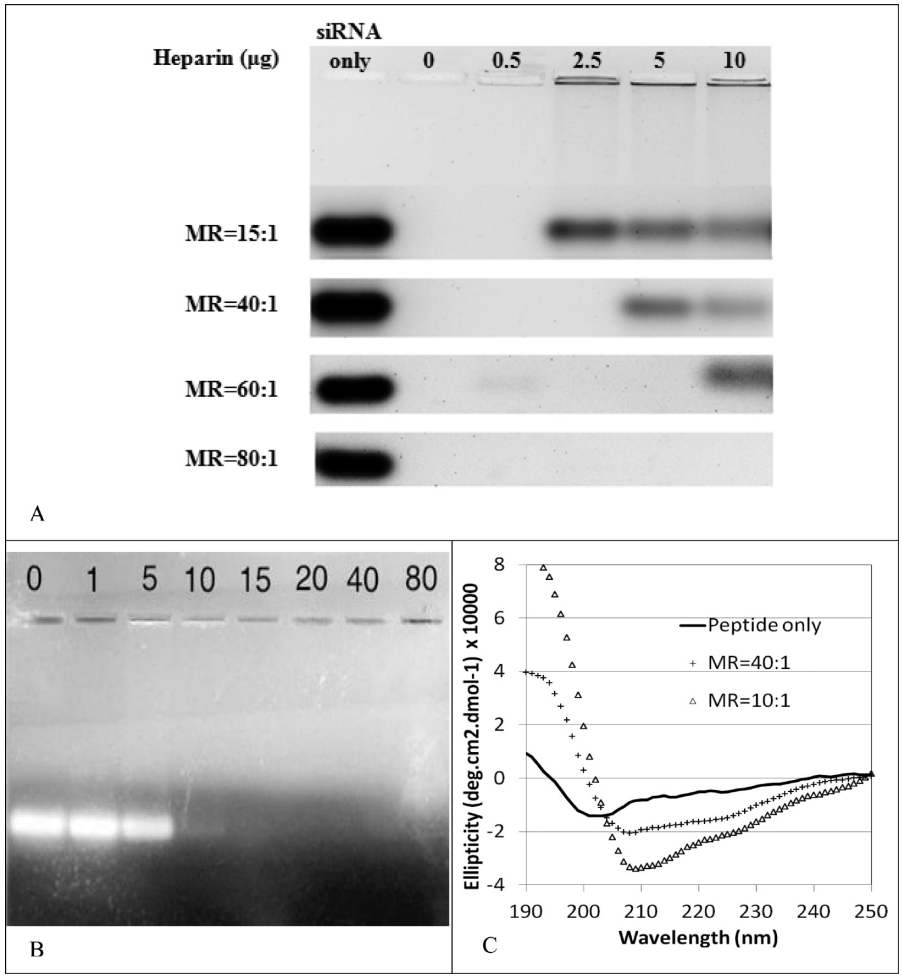

Figure 4. (A) Stability of C6−siRNA complex indicated by heparin competition assay. Different amounts of heparin corresponding to final concentrations of 0.5 to 10 μg heparin per 10 μL of complex were added to C6/siRNA complexes at different molar ratios. The stability of complexes was analyzed by electrophoresis on agarose gel (1.2 wt %/vol) stained with ethidium bromide. For better comparison, the siRNA bands of four independent gels were put in the same image. (B) Formation of C6-siRNA complexes at different molar ratios, indicated by agarose gel. SiRNA was incubated with different concentrations of C6 corresponding to a molar ratio ranging from 1:1 to 80:1. Lane 1 refers to siRNA control in the absence of C6, and lanes 2−8 refer to different molar ratios. (C) Secondary structure of peptide C6 (20 μM) alone and in complex with siRNA at molar ratios of 40:1 and 10:1, obtained by far-UV CD spectroscopy.

peptides are theoretically required to neutralize electrostatically one molecule of siRNA. Further experiments showed that the excess peptide molecules can provide a shield to protect siRNA molecules against degradation and also interact with cell membrane to initiate the peptide−siRNA cellular uptake.

The stability of C6-siRNA complexes at different molar ratios in the presence of heparin was also analyzed by gel electrophoresis. As shown in Figure 4A, C6-siRNA complexes were stable in the absence of heparin (second well from left), and no free siRNA was shown in siRNA bands at all MRs. The complex at MR of 15:1 was stable at very low concentration of heparin, that is, 0.5 μg per 10 μL of sample, but dissociated at higher heparin concentration. The minimum concentration of heparin required for dissociation of the complex increased by increasing the MR up to 60:1. However, the complex at the molar ratio of 80:1 was completely stable even at high heparin concentration (10 μg in 10 μL of loaded sample).

Conformational Changes of C6 upon Coassembling with siRNA. The impact of siRNA on the secondary structure of C6 was evaluated by CD spectroscopy. As reported in Figure 4C, C6 in water showed a small content of a random coil conformation with a minimum at 203 nm. By adding a small amount of siRNA (MR of 40:1), a clear shift in the spectrum minimum from 203 to 208 along with a maximum around 190 nm was observed, which represents a typical helical conformation. The absolute values of the minima at 208 and 222 nm and the maximum at 190 nm were increased by adding more siRNAs to MR of 10:1, which indicates the increase in helical content in secondary structure of the peptide at a higher concentration of siRNA. Adding further siRNA beyond the MR of 10:1 did not significantly change the secondary structure of the peptide (not shown), indicating a saturation point, as also observed in the gel electrophoresis and ITC tests. Considering the nature of C6 and siRNA interaction, that is, ionic interaction, the charge neutralization of seven arginine residues in the peptide sequence may decrease the repulsion between them, which eventually facilitated the peptide adoption to a helical conformation.

Fluorescence Spectroscopy. The formation of siRNA/C6 complexes was also evaluated by intrinsic fluorescence spectroscopy, using the Trp residue in C6 as the internal fluorescent probe to monitor the interaction with siRNA. As

dx.doi.org/10.1021/jp3072553 | J. Phys. Chem. B 2012, 116, 13183−13191

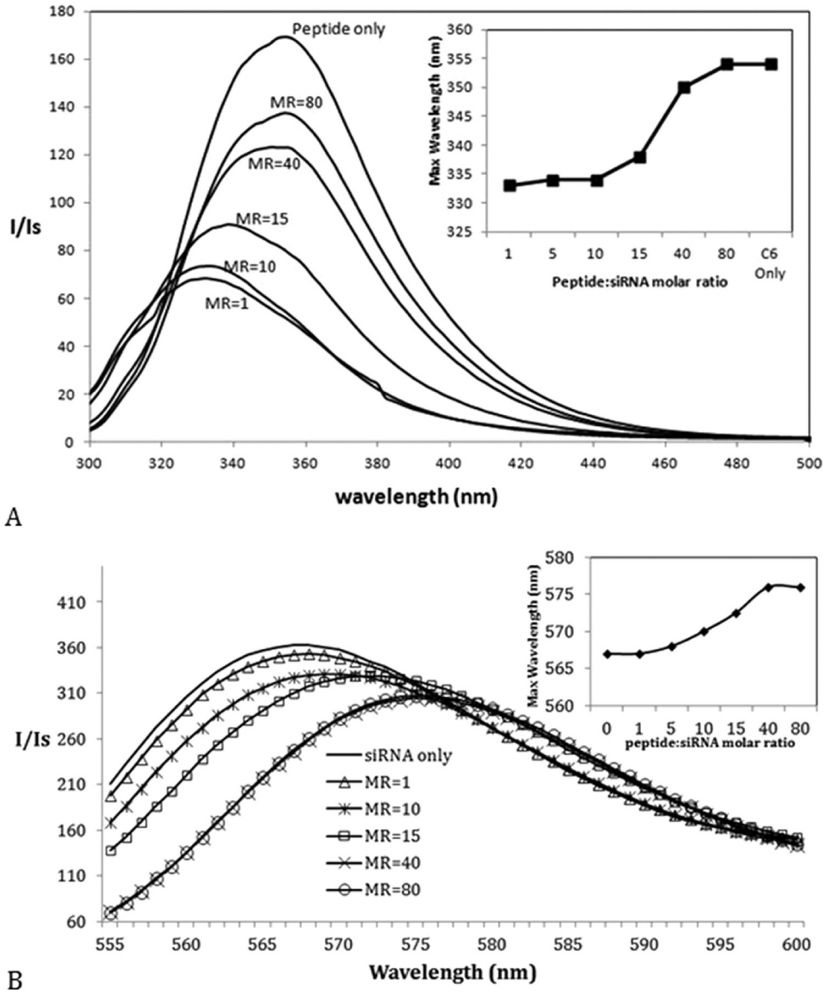

Figure 5. C6−siRNA interaction monitored by fluorescence spectroscopy. (A) Intrinsic Trp fluorescence of C6 was excited at 280 nm, and the emission spectra were recorded from 300 to 500 nm. A fixed concentration of 160 nM of peptide was titrated by increasing siRNA concentration from molar ratio 80/1 to 1/1. (B) Cy-3 labeled siRNA was used as extrinsic fluorescent probe, and the change in fluorescence spectra was studied at a fixed concentration of siRNA (2 μM) and increasing concentration of peptide to achieve different molar ratios. The samples were excited at 540 nm, and spectra were collected in the range of 550−800 nm.

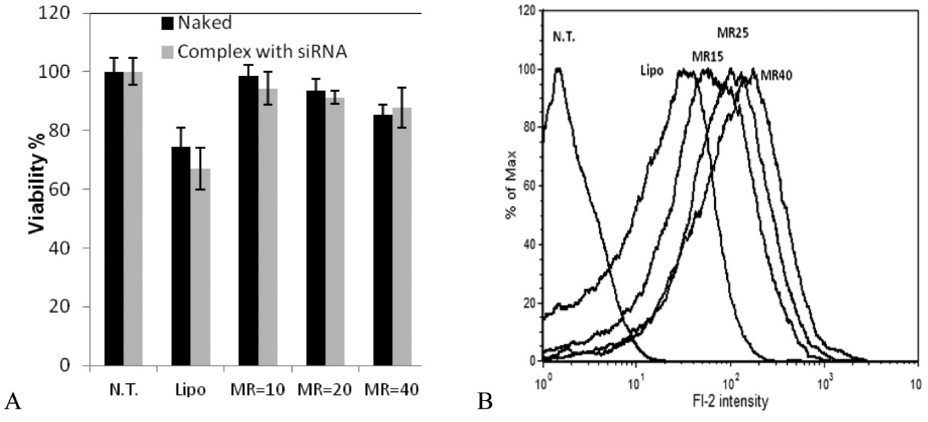

Figure 6. (A) Cytotoxicity of peptide C6 in complex with siRNA (50nM) at different molar ratios or peptide alone at the same concentrations. (N.T. = nontreated, MR = peptide/siRNA molar ratio). (B) Flow cytometry results for Cy3-labeled siRNA delivered by lipofectamin and C6 at different molar ratios (MRs).

shown in Figure 5A, the peptide-only sample had an emission peak at 354 nm. The binding of C6 to siRNA from molar ratio of 80:1 to 1:1 induced quenching of Trp fluorescence as well as a blue shift in maximum spectra. As shown in Figure 5A, at the molar ratio of 10:1, 55% quenching of fluorescence, accompanied by a 20 nm blue shift from 354 to 334 nm (Figure 5A, inset), was observed. No significant change in fluorescence intensity and peak wavelength was observed by

dx.doi.org/10.1021/jp3072553 | J. Phys. Chem. B 2012, 116, 13183−13191

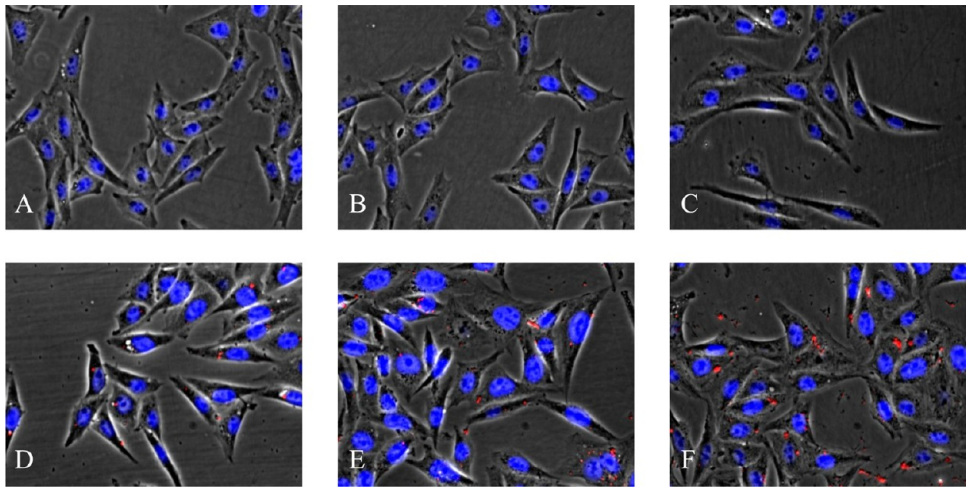

Figure 7. Subcellular distribution pattern of Cy3-labeled siRNA 3 h post-treatment. Cy3-labeled GAPDH siRNA (red) was transfected to CHO cells with positive control reagent and different molar ratio of C6 at a concentration of 50nM. Cells were analyzed by fluorescence microscopy 3 h after transfection (magnification, 40×). Nuclei were stained with DAPI (blue). (A) Nontreated cells and (B) cells treated with 50 nM siRNA only, (C) with C6 peptide only, (D) with Lipofectamine 2000 as positive control, and (E) with siRNA complexed with C6 at molar ratio of 15:1and (F) molar ratio of 40:1.

adding more siRNAs (e.g., at MR = 1:1), which indicates a saturation in peptide−siRNA interaction at MR = 10:1. This finding is in agreement with what is reported in agarose gel assay. The blue shift signifies a change in the environment of Trp residue from polar to nonpolar, indicating a conformational change of C6 upon interaction with siRNA, as also confirmed by CD.[36]

Similarly, the interaction of C6 with labeled siRNA induced a red shift along with quenching in maximum spectra of extrinsic Cy-3 label of siRNA, starting from molar ratio of 10:1 (Figure 5B). The red shift and quenching reached their maximum of 10 nm and 15%, respectively, at molar ratio of 40:1 because adding more peptide did not change the spectra (MR = 80:1). This may suggest that the extra peptides did not interact with the preformed C6-siRNA complexes. Considering the results of all performed characterization experiments, a C6:RNA molar ratio between 15:1 and 40:1 was suggested to perform transfection experiments.

Cytotoxicity of Peptide−siRNA Complex. Cell viability studies were performed, using the CCK-8 assay, on CHO-K1 cells. As shown in Figure 6A, no significant difference was observed in the viability of cells treated with C6-siRNA complexes or C6-only samples at the same concentration. None of the peptide−siRNA samples showed considerable toxicity on CHO cells because the viability of the cells was not reduced below 85%, even at molar ratio of 40:1. However, the cells treated with Lipofectamine showed significant toxicity. These results clearly show that peptide C6 can be used as a safe siRNA delivery carrier with lower cytotoxicity, compared with commonly used lipid-based reagents.

Cellular Uptake of Peptide−siRNA Complex. The efficiency of C6 to deliver siRNA into CHO cells was evaluated using FACS. As shown in Figure 6B, cellular uptake efficiency of siRNA was correlated to the molar ratio of C6-siRNA. Even though a 15:1 molar ratio was sufficient to deliver an even higher amount of siRNA into cells compared with lipofectamine 2000, the intracellular fluorescence intensity increased with increasing molar ratio (MR25 and MR40).

To study the cellular uptake, distribution, and localization of siRNA complexed with C6, we transfected CHO cells with Cy3-labeled siRNA alone or in complex with C6 or lipofectamine 2000. CHO cells were incubated with or without complexes for 3 h and observed under a fluorescence microscope (Figure 7).

As expected, Cy-3 siRNA alone was not able to enter the cells by itself due to the negative charge and lack of an appropriate delivery vector (Figure 7B). siRNA internalization happened within 3 h of incubation at the present of transfection reagent, lipofectamine 2000, as shown as small red dots in the cytosol of most of the cells (Figure 7D). In the cells treated with C6-siRNA complexes (Figure 7E,F), siRNA was localized to regions in close proximity to the nuclear membrane. siRNAs delivered by C6 showed a punctual nonhomogeneous distribution pattern around the periphery of the nucleus inside the cell, which indicated the possibility of endocytosis pathways.[37] Further research to study the uptake mechanism of this family of peptides is currently in progress.

C6-siRNA complexes at high molar ratios (MR = 40:1) may form high-molecular-weight complexes or aggregate, as previously documented for other CPPs. These large complexes may be internalized through the macropinocytosis pathway, which can include all pinosomes larger than 200 nm.[13] However the uptake of large aggregates by fluid phase endocytosis may not result in the effective release of siRNA into the cytoplasm and eventually significant gene knockdown. Thus, precautions should be taken into account while increasing the molar ratio because the large aggregates might have problems dissociating and releasing siRNA in the cells, eventually decreasing the knockdown efficiency of the complex.

■ CONCLUSIONS

C6, an amphipathic, AAP peptide, was introduced as a safe and efficient carrier for siRNA delivery in vitro. The noncovalent interaction/coassembly between C6 and siRNA and the physicochemical properties of the resulting coassemblies were studied. C6 alone showed a random coil secondary structure in water but adopted a helical conformation upon binding to siRNA. The ITC results showed an entropy-driven interaction between C6 and siRNA with stoichiometry of 6.5, which was close to the theoretical value of 6, required for charge

neutralization. The gel electrophoresis, fluorescence spectroscopy, DLS, and AFM results confirmed stable C6-siRNA complex formation in the molar ratios from 10:1 to 40:1. The flow cytometry data and fluorescence microscopy images also indicated the high cellular uptake and cytoplasmic localization of siRNA delivered by C6. Considering these results and the fact that C6 is nontoxic at the concentrations used, this peptide demonstrated potential as an efficient carrier for siRNA delivery.

AUTHOR INFORMATION

Corresponding Author

*Tel: +1 519-888-4567, ext. 35586. Fax: 1-519-888-4347. E-mail: p4chen@uwaterloo.ca.

Author Contributions

‖These authors contribute equally

Notes

The authors declare no competing financial interest.

ACKNOWLEDGMENTS

We are grateful for the financial support from the Natural Sciences and Engineering Research Council of Canada (NSERC), the Canadian Foundation for Innovation (CFI), Waterloo Institute of Nanotechnology (WIN), and the Canadian Research Chairs (CRC) program.

REFERENCES

(1) Fire, A.; Xu, S. Q.; Montgomery, M. K.; Kostas, S. A.; Driver, S. E.; Mello, C. C. *Nature* **1998**, *391*, 806−811.
(2) Lee, M.; Kim, S. W. *Pharm. Res.* **2005**, *22*, 1−10.
(3) Huang, S. W.; Zhuo, R. X. *Chin. Sci. Bull.* **2003**, *48*, 1304−1309.
(4) Jeong, J. H.; Park, T. G. *J. Controlled Release* **2002**, *82*, 159−166.
(5) Wasungu, L.; Hoekstra, D. *J. Controlled Release* **2006**, *116*, 255−264.
(6) Rao, N. M.; Gopal, V. *Biosci. Rep.* **2006**, *26*, 301−324.
(7) Ilies, M. A.; Balaban, A. T. *Expert Opin. Ther. Pat.* **2001**, *11*, 1729−1752.
(8) Veldhoen, S.; Laufer, S. D.; Restle, T. *Int. J. Mol. Med.* **2008**, *9*, 1276−1320.
(9) Deshayes, S.; Decaffmeyer, M.; Brasseur, R.; Thomas, A. *Biochim. Biophys. Acta, Biomembr.* **2008**, *1778*, 1197−1205.
(10) Crombez, L.; Charnet, A.; Morris, M. C.; Aldrian-Herrada, G.; Heitz, F.; Divita, G. *Biochem. Soc. Trans.* **2007**, *35*, 44−46.
(11) Jafari, M.; Chen, P. *Curr. Top. Med. Chem.* **2009**, *9*, 1088−1097.
(12) Crombez, L.; Aldrian-Herrada, G.; Konate, K.; Nguyen, Q. N.; McMaster, G. K.; Brasseur, R.; Heitz, F.; Divita, G. *Mol. Ther.* **2009**, *17*, 95−103.
(13) Jones, A. T. *J. Cell. Mol. Med.* **2007**, *11*, 670−684.
(14) Richard, J. P.; Melikov, K.; Brooks, H.; Prevot, P.; Lebleu, B.; Chernomordik, L. V. *J. Biol. Chem.* **2005**, *280*, 15300−15306.
(15) Hirose, H.; Takeuchi, T.; Osakada, H.; Pujals, S.; Katayama, S.; Nakase, I.; Kobayashi, S.; Haraguchi, T.; Futaki, S. *Mol. Ther.* **2012**, *20*, 984−993.
(16) Konate, K.; Crombez, L.; Deshayes, S.; Decaffmeyer, M.; Thomas, A.; Brasseur, R.; Aldrian, G.; Heitz, F.; Divita, G. *Biochemistry* **2010**, *49*, 3393−3402.
(17) Deshayes, S.; Plenat, T.; Aldrian-Herrada, G.; Divita, G.; Grimmellec, C. D.; Heitz, F. *Biochemistry* **2004**, *43*, 7698−7706.
(18) Lundberg, P.; Magzoub, M.; Lindberg, M.; Hallbrink, M.; Jarvet, J.; Eriksson, L. E. G.; Langel, U.; Graslund, A. *Biochem. Biophys. Res. Commun.* **2002**, *299*, 85−90.
(19) Fung, S.; Yong, H.; Sadatmousavi, P.; Sheng, Y.; Mamo, T.; Nazaian, R.; Chen, p. *Adv. Func. Mater.* **2011**, *21*, 2456−2464.
(20) Sadatmousavi, P.; Soltani, M.; Nazarian, R.; Jafari, M.; Chen, P. *Curr. Pharm. Biotechnol.* **2011**, *12*, 1089−1100.
(21) Wang, M.; Law, M.; Duhamel, J.; Chen, P. *Biophys. J.* **2007**, *93*, 2477−2490.
(22) Law, M.; Jafari, M.; Chen, P. *Biotechnol. Prog.* **2008**, *24*, 957−963.
(23) Nakase, I.; Tadokoro, A.; Kawabata, N.; Takeuchi, T.; Katoh, H.; Hiramoto, K.; Negishi, M.; Nomizu, M.; Sugiura, Y.; Futaki, S. *Biochemistry* **2007**, *46*, 492−501.
(24) Futaki, S.; Suzuki, T.; Ohashi, W.; Yagami, T.; Tanaka, S.; Ueda, K.; Sugiura, Y. *J. Biol. Chem.* **2001**, *276*, 5836−5840.
(25) Chou, P. Y.; Fasman, G. D.; Chou, P. Y.; Fasman, G. D. *J. Mol. Biol.* 1973, *74*, 263−281.
(26) Langel, Ü. In *Handbook of Cell-Penetrating Peptides*; Taylor & Francis: Boca Raton, FL, 2007.
(27) Maeda, H.; Wu, J.; Sawa, T.; Matsumura, Y.; Hori, K. *J. Controlled Release* **2000**, *65*, 271−284.
(28) Fang, J.; Nakamura, H.; Maeda, H. *Adv. Drug Delivery Rev.* **2011**, *63*, 136−151.
(29) Torchilin, V. *Adv. Drug Delivery Rev.* **2011**, *63*, 131−135.
(30) Rejman, J.; Oberle, V.; Zuhorn, I. S.; Hoekstra, D. *Biochem. J.* **2004**, *377*, 159−169.
(31) Benoit, J.; Vonarbourg, A.; Passirani, C.; Saulnier, P. *Biomaterials* **2006**, *27*, 4356−4373.
(32) Mahato, R. I. In *Biomaterials for Delivery and Targeting of Proteins and Nucleic Acids*; CRC Press: Boca Raton, FL, 2005.
(33) Jun, S.; Hong, Y.; Imamura, H.; Ha, B.; Bechhoefer, J.; Chen, P. *Biophys. J.* **2004**, *87*, 1249−1259.
(34) Stolarski, R. *Acta Biochim. Pol.* **2003**, *50*, 297−318.
(35) Klump, H. *Biophys. Chem.* **1976**, *5*, 363−367.
(36) Zhou, T.; Rosen, B. *FASEB J.* **1997**, *11*, A1147−A1147.
(37) Veldhoen, S.; Laufer, S. D.; Trampe, A.; Restle, T. *Nucleic Acids Res.* **2006**, *34*, 6561−6573.